

**In-medium  $\rho^0$  spectral function  
study via the  
 $^2\text{H}$ ,  $^3\text{He}$ ,  $^{12}\text{C}(\gamma, \pi^+ \pi^-)$  reaction**

**G.M. Huber**

*University of Regina  
Regina, SK Canada*

PRC **68** (2003) 065202.

## The TAGX Collaboration

G.M. Huber, G.J. Lolos, Z. Papandreou, A. Shinozaki, E.J. Brash, M. Iurescu  
*Department of Physics, University of Regina, Regina, SK, S4S 0A2, Canada*

G. Garino, K. Maruyama  
*Institute for Nuclear Study, University of Tokyo, Tanashi, Tokyo 188, Japan*

K. Maeda, T. Suda, A. Toyofuku  
*Department of Physics, Tohoku University, Sendai 980, Japan*

B.K. Jennings  
*TRIUMF, Vancouver, BC, V6T 2A3, Canada*

A. Sasaki  
*College of General Education, Akita University, Akita 010, Japan*

H. Yamashita  
*Department of Applied Physics, Tokyo University of Agriculture and Technology,  
Koganei, Tokyo 184, Japan*

## Medium modifications of light hadrons

One of the central properties of QCD in the nonperturbative region is the spontaneous breaking of chiral symmetry in the ground state, resulting in a nonvanishing chiral condensate,  $\langle q\bar{q} \rangle \neq 0$ .

- Many QCD-based calculations suggest that the masses and couplings of light hadrons are controlled by chiral symmetry and its breaking.  
⇒ Confinement seems to play a lesser role.
- Hadronic properties should depend on the value of the chiral condensate  $\langle q\bar{q} \rangle$ .
- Hadronic properties should be modified in the nuclear medium, where the chiral condensate is reduced.
- Lattice QCD calculations suggest that chiral symmetry will be restored at  $T_c \geq 150$  MeV and/or  $\rho_c \geq 5 \rho_{nuc}$ .  
⇒ expect significant hadronic property modifications near these values.

By investigating medium effects on hadronic properties, one can test our understanding of those nonperturbative aspects of QCD which are responsible for the light hadronic states.

## Of all particles, the $\rho^0$ has received the most attention with regard to medium modifications.

- Since the  $\rho^0$  carries the quantum numbers of the conserved vector current ( $J^{PC} = 1^{--}$ ), its properties are related to chiral symmetry.
- Can be investigated with effective chiral models, current algebra, QCD Sum Rules, etc.  
Brown & Rho scaling [PRL **66** (1991) 2720]

$$\frac{m_N^*}{m_N} \approx \frac{m_\rho^*}{m_\rho} \approx \frac{m_\omega^*}{m_\omega} \approx \frac{f_\pi^*}{f_\pi}$$

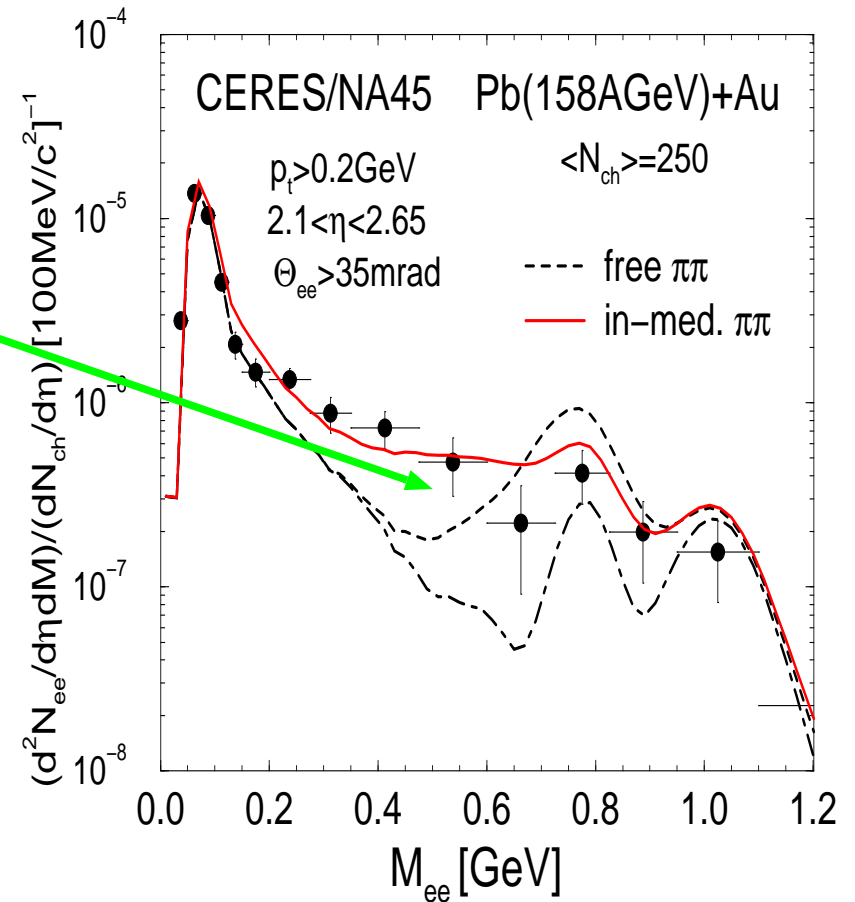
- based on chiral symmetry arguments and scale invariance.
- $m_\rho$  should drop from its free value by  $\sim 15\%$  at normal  $\rho_{nuc}$ .
- Lattice QCD calculations suggest that  $m_\rho$  should drop by  $\sim 25\%$  at normal  $\rho_{nuc}$ .  
[Jin & Leinweber, PRC **52** (1995) 3344]

These predictions are complicated by the presence of the nuclear medium, as one must try to disentangle conventional in-medium effects from those which may be due to the change of the chiral condensate.

Experimental evidence for  $\rho^0$  mass modification has been widespread, but all suffer from significant model uncertainties.

- CERN dilepton production data from  $S+Au$  and  $S+W$  collisions at 200 GeV/u yield a significant enhancement at low  $m_{ee}$ .

➔ Density-dependent mass reduction consistent with Chiral symmetry restoration as well as with  $\rho$ -medium scattering.



[A. Drees et al., NP **A610** (1996) 536c.]

## Experimental evidence

- IUCF  $^{28}\text{Si}(\vec{p}, \vec{p}')^{28}\text{Si}$  polarization transfer data found an effective isovector  $NN$  interaction strength consistent with  $m_\rho \approx 615$  MeV.

[Stephenson et al., PRL **78** (1997) 1636].

- TAGX  $^3\text{He}(\gamma, \pi^+\pi^-)ppn$  production data utilizing Fermi momentum to produce  $\rho^0$  in the subthreshold region found an energy-dependent mass reduction  $m_\rho \approx 640 - 680$  MeV.

[Lolos et al., PRL **80** (1998) 241, Kagarlis et al., PRC **60** (1999) 025203].

- Frascati  $\gamma A$  total photoabsorption cross sections on  $C, Al, Cu, Sn, Pb$  at 0.5-2.6 GeV are less than expected (i.e. more shadowing).

Best explained in terms of reduced in-medium  $m_\rho \sim 610 - 710$  MeV.

$\Rightarrow$  increases coherence length  $\lambda_\rho = 2k/m_\rho^2$ .

$\Rightarrow$  decreases threshold for shadowing.

The size of the required mass shift is inversely proportional to  $A$ .

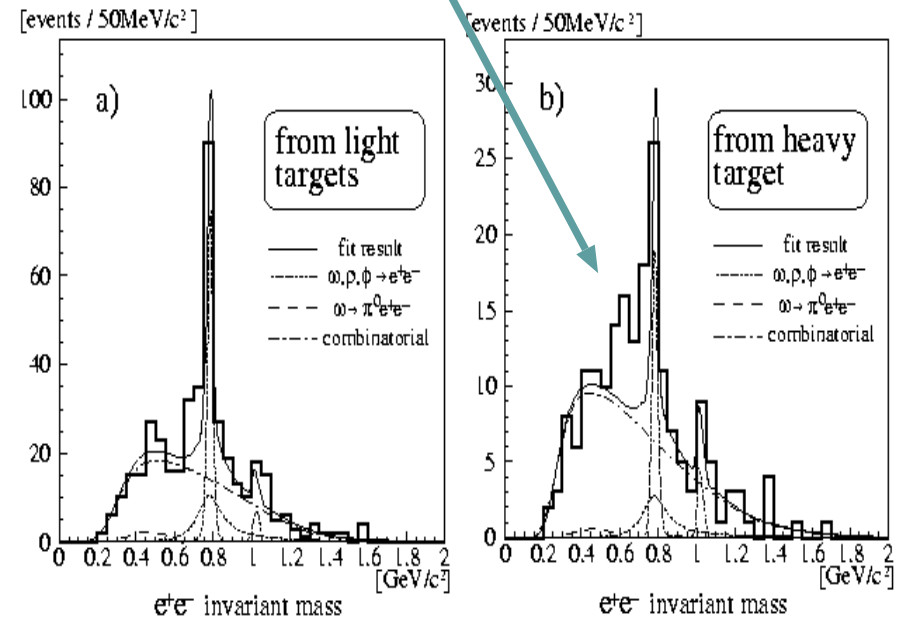
[Bianchi et al., PRC **60** (1999) 064617].

# Experimental evidence

- KEK  $e^+e^-$  spectra obtained from 12 GeV  $p+A$  collisions yield a significant enhancement on  $Cu$  which is not present on  $^{12}C$ .

⇒ Consistent with  $\approx 200$  MeV  $\rho/\omega$  mass shift.

[Ozawa et al., PRL **86** (2001) 5019.]



There is a need for data which can be interpreted in a less model-dependent fashion.

# Important Aspects of our $A(\gamma, \pi^+ \pi^-)$ Experiment

Choose the “subthreshold” region to maximize nuclear interaction effect

⇒ require Fermi momentum to put  $\rho^0$  on shell.

⇒  $\rho^0$  produced with low boost with respect to nuclear medium.

⇒ suppresses diffractive  $\rho^0$  production.

960-1120 MeV

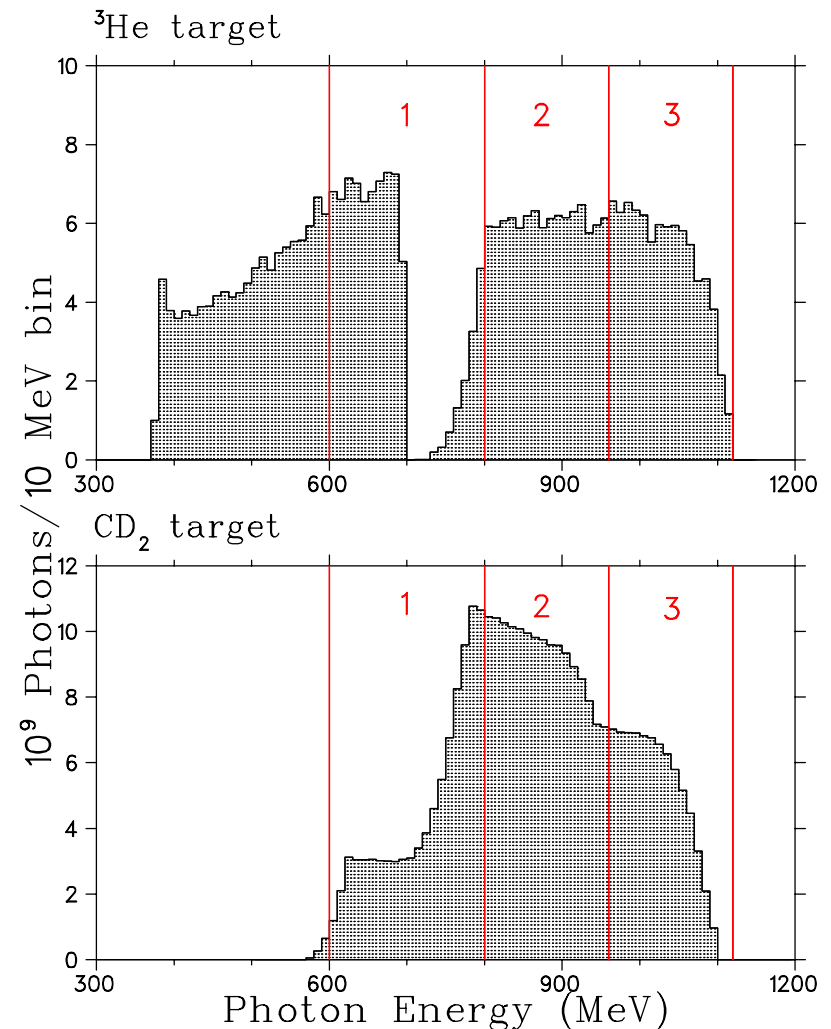
Above threshold for  $^1H$  target.

800-960 MeV

Subthreshold for  $^1H$  target.

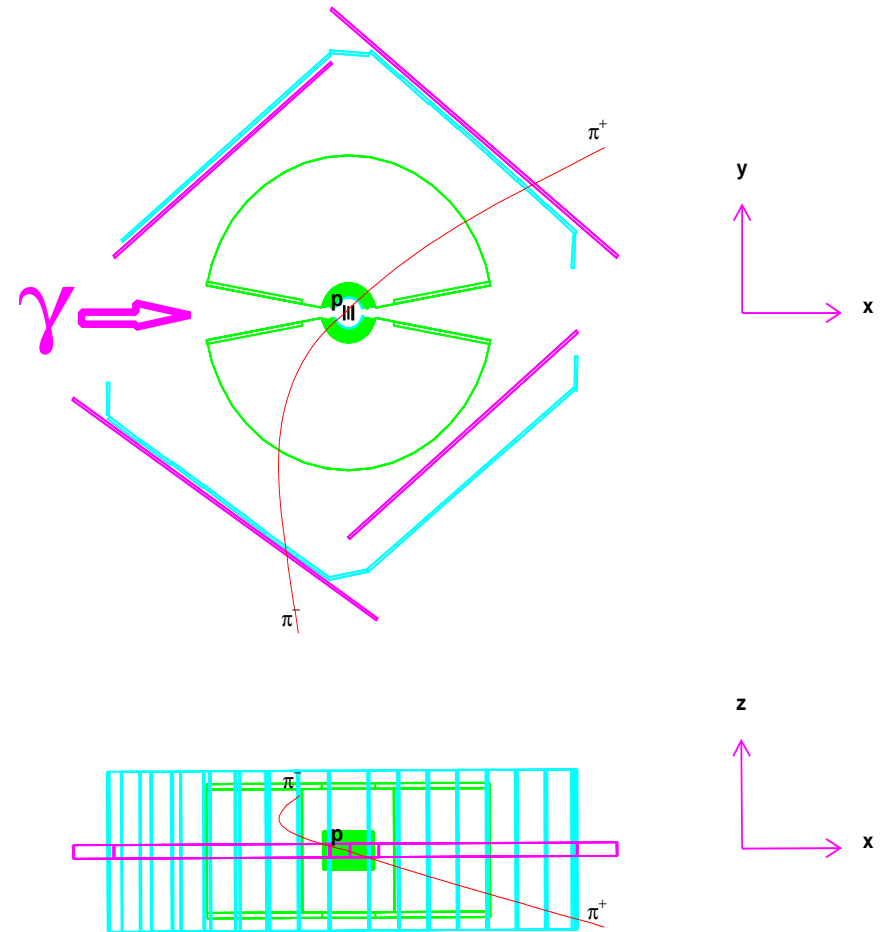
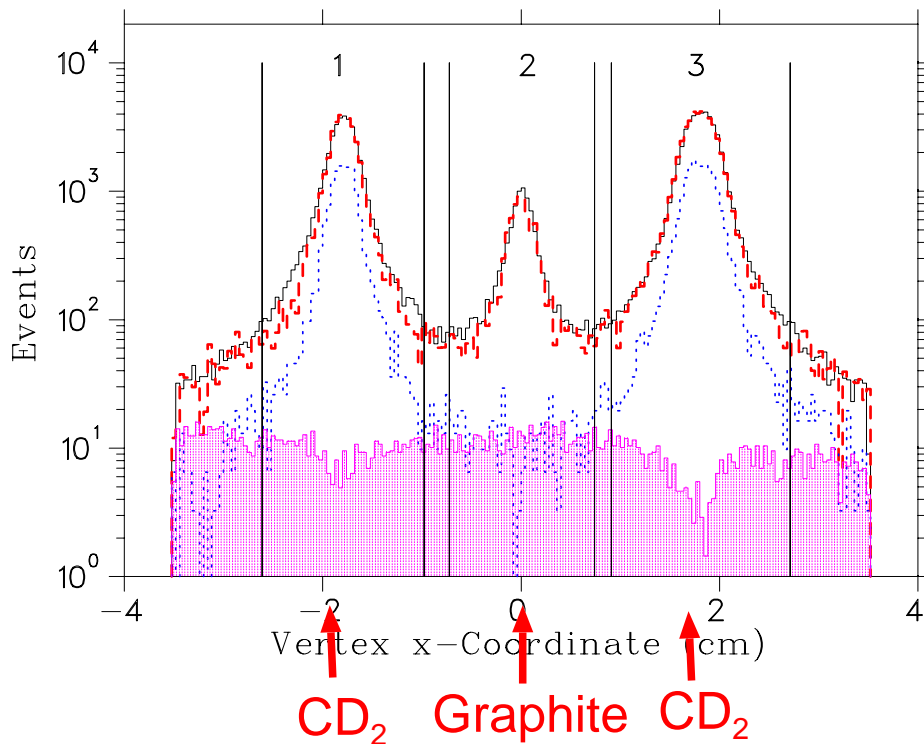
600-800 MeV

Deeply subthreshold for nuclear target.

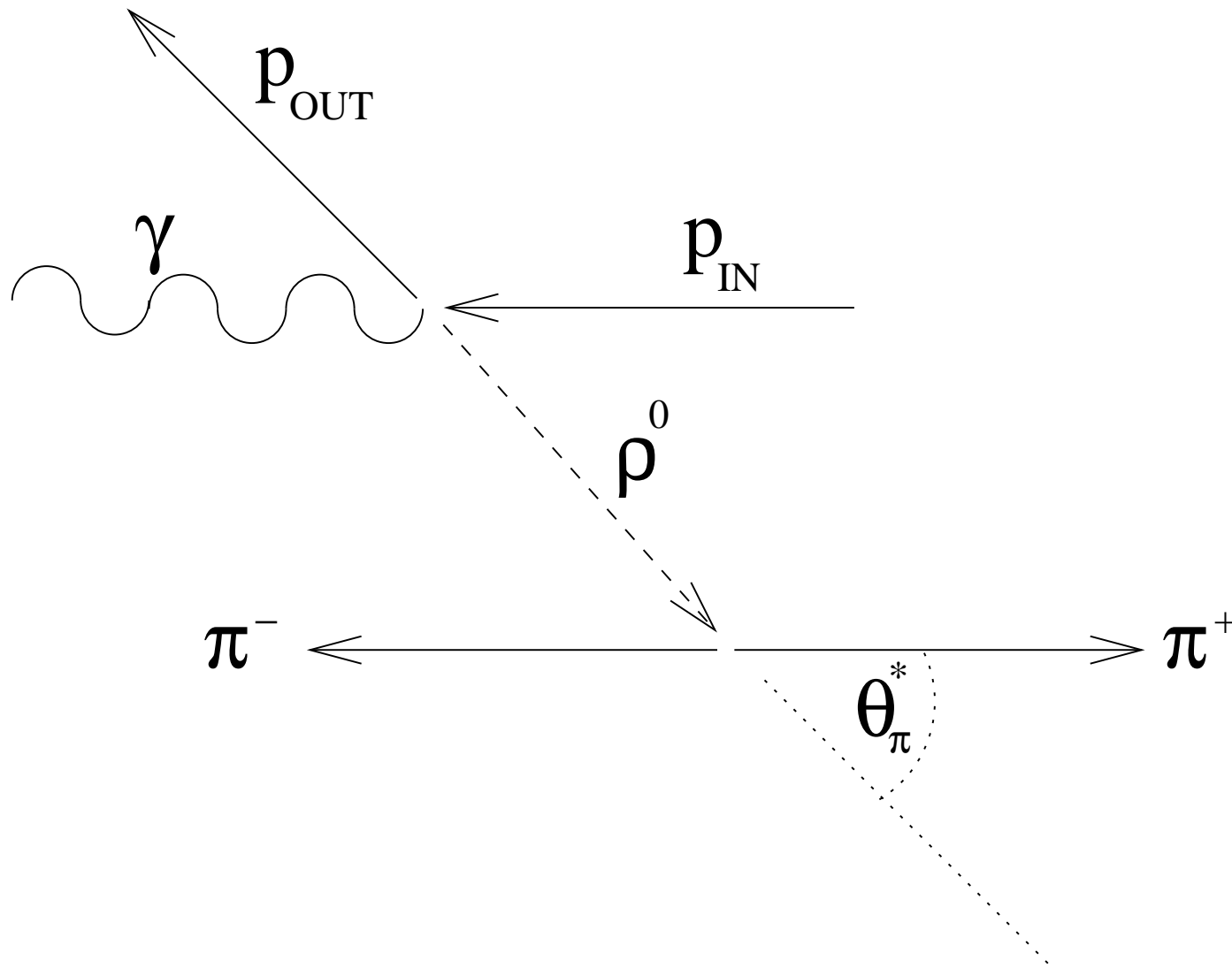


# Detect $\pi^+\pi^-$ in TAGX large angle spectrometer

- ⇒ 1  $\pi$  sr, horizontal acceptance optimized for planar detection of particles emitted with large opening angle.
- ⇒  $\rho^0 \rightarrow \pi^+\pi^-$  decay channel has favorable  $\approx 100\%$  decay ratio.
- ⇒ minimize  $\pi$ -N FSI by choice of nucleus ( ${}^2\text{H}$ ,  ${}^3\text{He}$ ,  ${}^{12}\text{C}$ ).

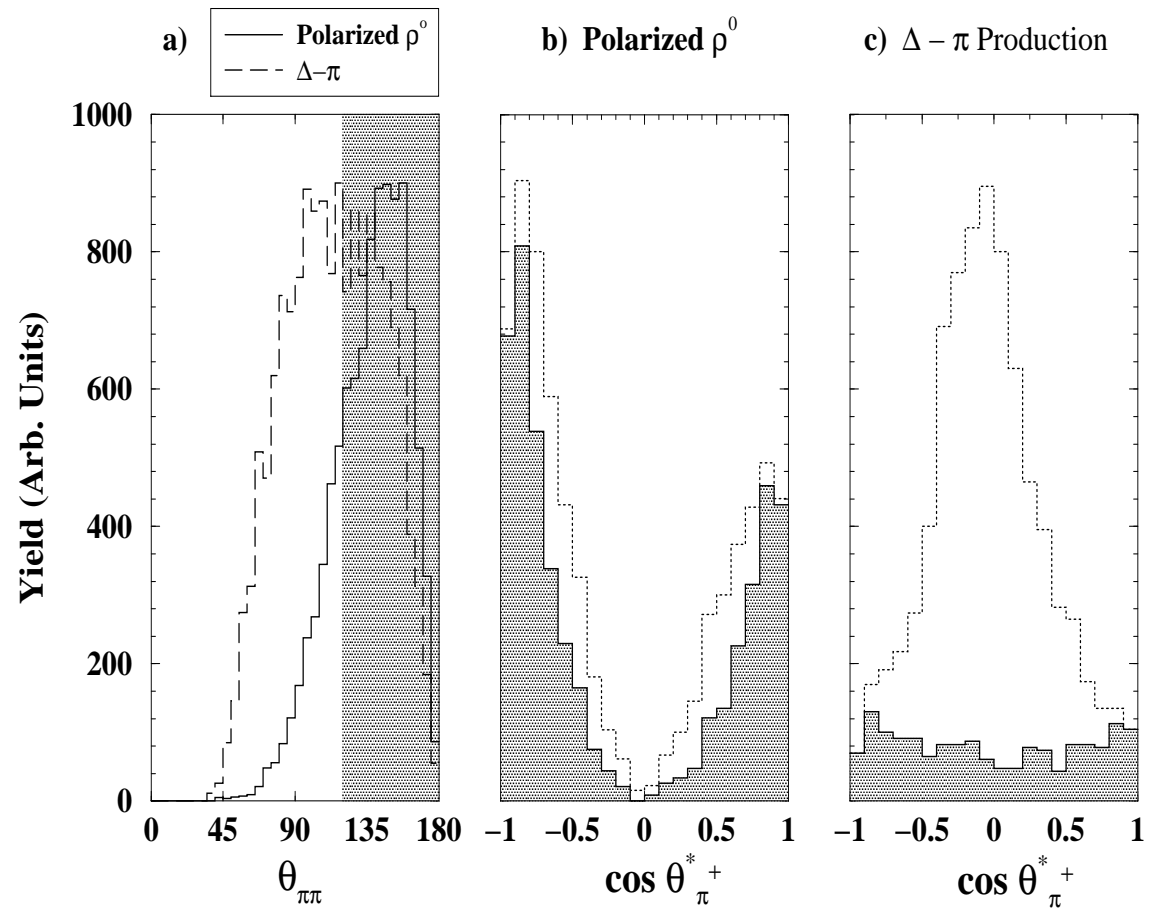
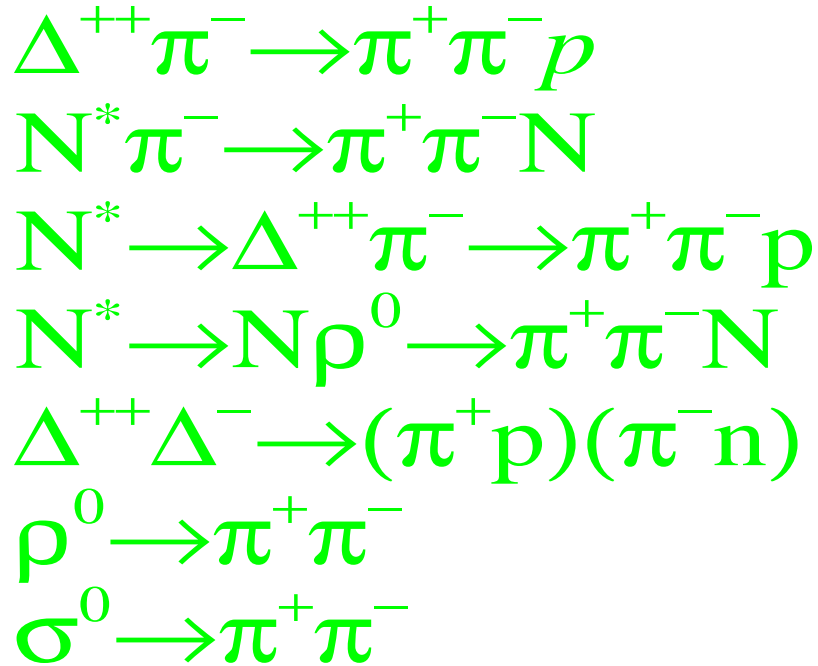


## Reconstruct the $\rho^0$ decay angular distribution



- Usually studied in the  $s$ -channel helicity frame.
- $\rho^0$  direction is taken as the quantization axis.
- $\theta^*$  is the polar angle of the  $\pi^+$  in the  $\rho^0 \rightarrow \pi^+\pi^-$  C.M. system.

There are many possible ways of producing a  $\pi^+\pi^-$  pair in this energy range.



To understand the  $A(\gamma, \pi^+\pi^-)$  data, it is necessary to take into account the presence of these processes.

$\Rightarrow$  MC simulations used to evaluate the effectiveness of various cuts upon the data.

# Simulated $\pi^+\pi^-$ production channels

## Quasi-free $\rho^0$ production.

- ◆ line shape taken from  $l=1$  partial wave analysis of  $e^+e^- \rightarrow \pi^+\pi^-$  data.

## Quasi-free $\sigma^0$ production.

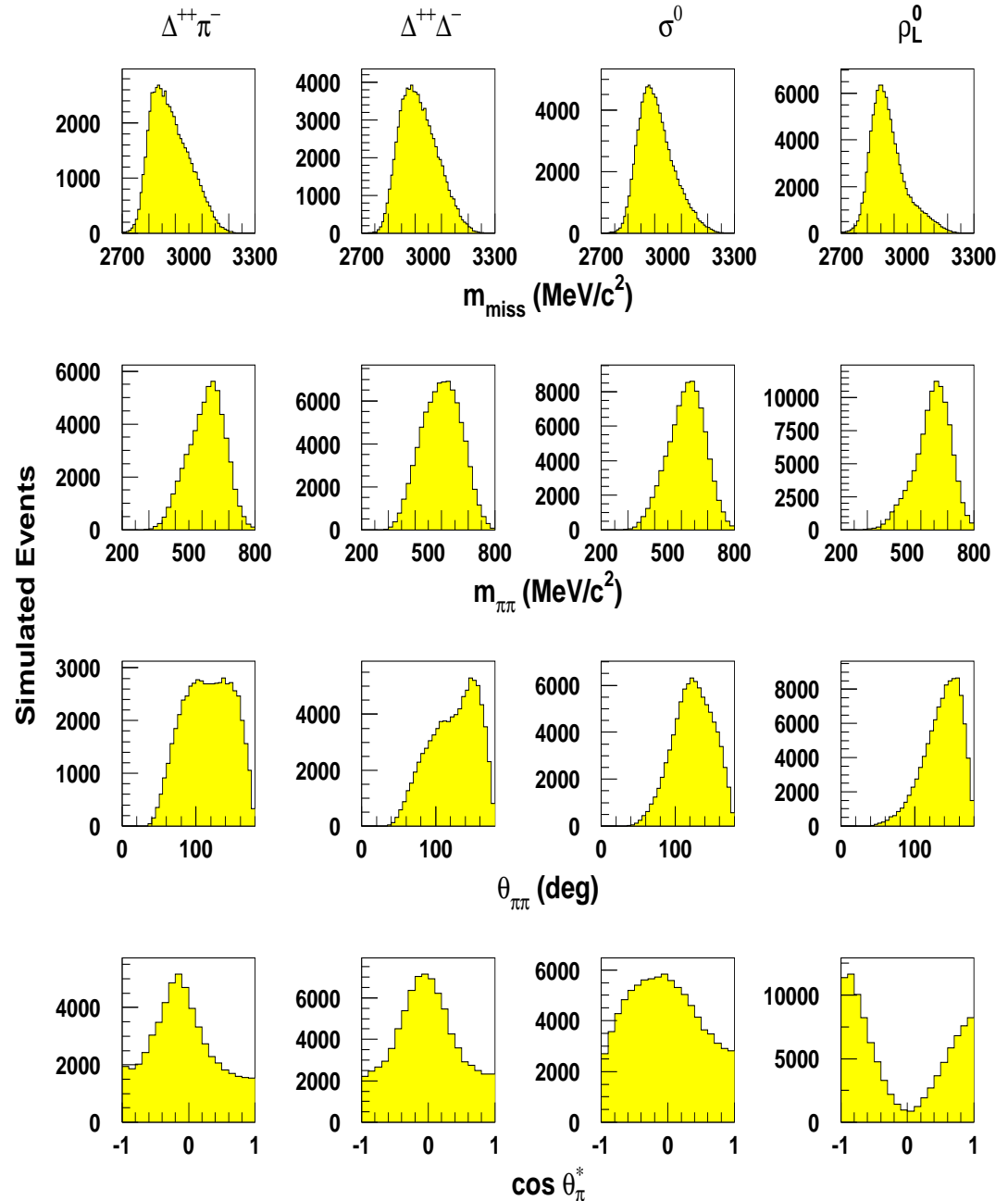
- ◆ similar to  $\rho^0$ , except  $l=0$ .
- ◆ used to investigate whether any cut-induced  $l=1$  signatures appear in the MC simulations.

## Quasi-free Baryon resonances.

- ◆  $\Delta^{++}\pi^-$ ,  $\Delta^-\pi^+$ ,  $N^*(1520)\pi^-$ ,  
 $N^*(1520) \rightarrow \Delta^{++}\pi^-$ ,  $N^*(1520) \rightarrow p\rho^0$ .
- ◆ missing-mass cut required to exclude  $>2\pi$  processes.
- ◆  $\Delta\Delta$  involves 2 nucleons, so is simulated as test case.

## $\pi N$ Final State Interactions (FSI).

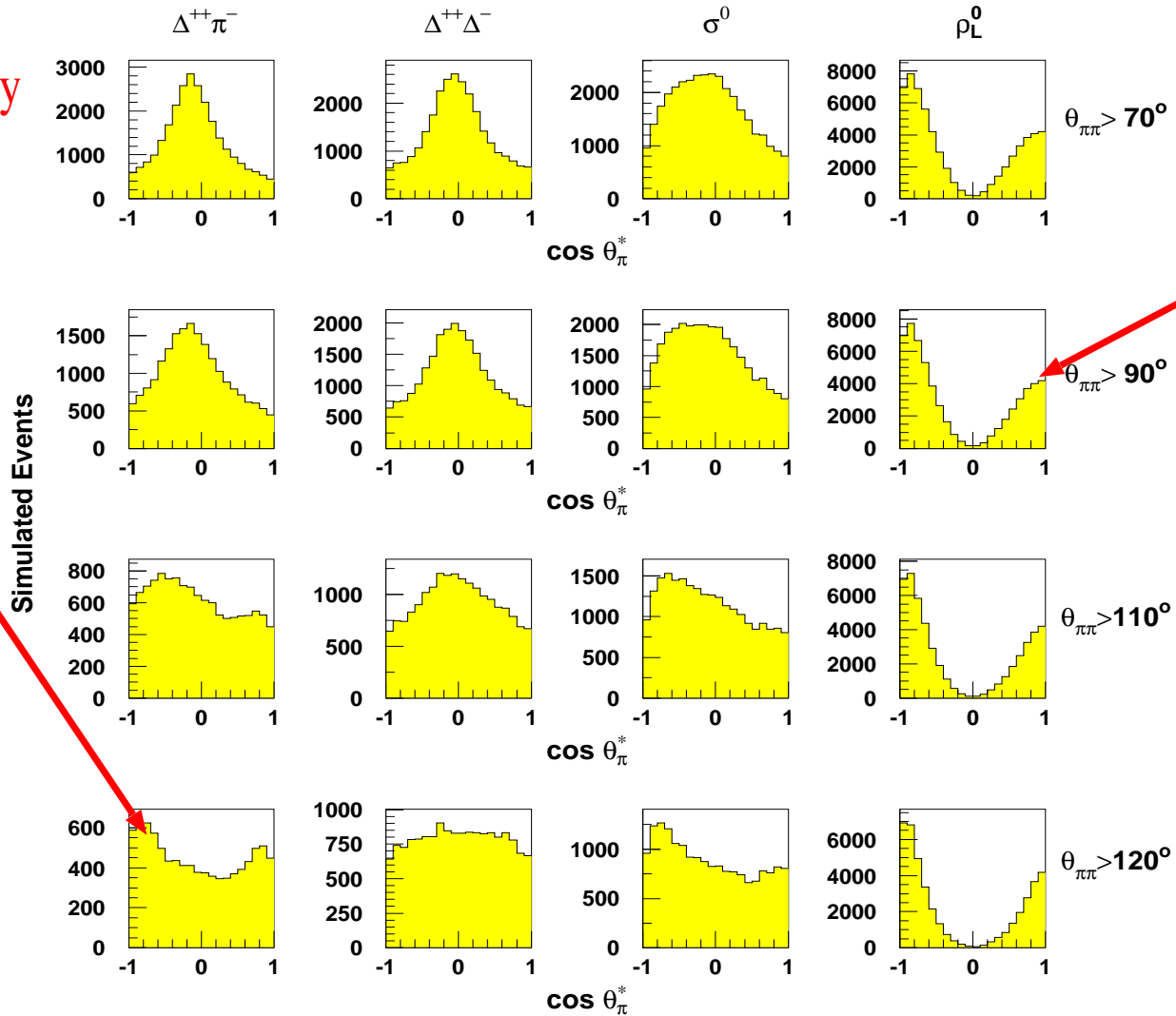
- ◆  $\pi + N_F \rightarrow \pi + N'$ .
- ◆  $\pi N$  amplitudes taken from phase shift analysis of Rowe, Salomon and Landau [PRC 18 (1978) 584].



${}^3\text{He}$ ,  $800 < E_\gamma \leq 960$  MeV

# Investigation of the effect of the opening angle $\theta_{\pi\pi}$ cut

Events are primarily cut from the edges of the distribution. Portions near  $\pm 1$  are unchanged.



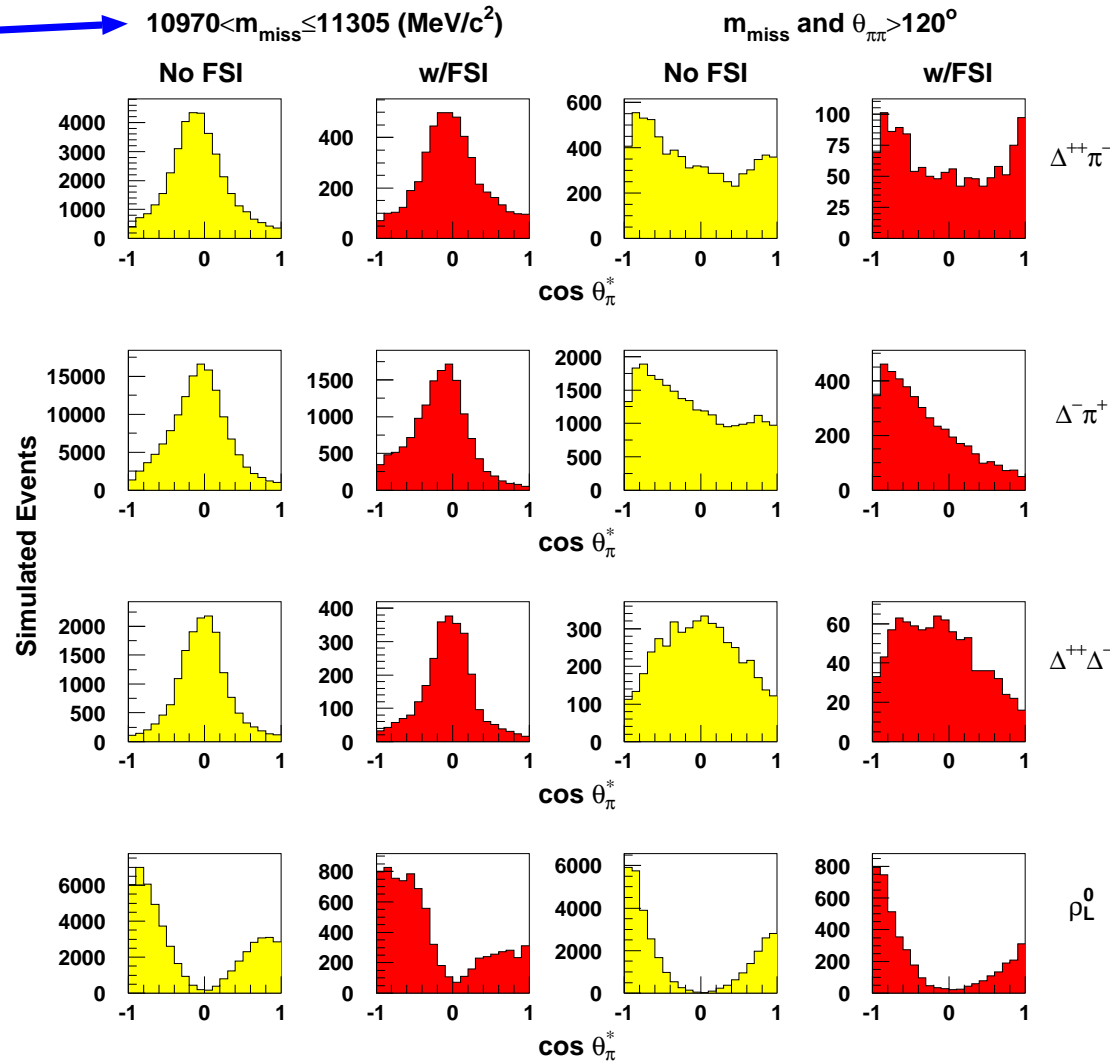
$\rho^0$  simulation maintains unique edge-to-center ratio.

The relative enhancement of  $\rho^0$  events is as much as a factor of 10.

The combination of  $m_{miss}$  and  $\theta_{\pi\pi}$  cuts enhance the relative proportion of  $\rho^0$  events in the data. They do not appear to induce a false  $\cos^2\theta$  distribution to the data.

# The effect of the cuts upon $\pi$ - $N$ FSI in $^{12}\text{C}$

$m_{\text{miss}}$  cut  $\longrightarrow$  10970 <  $m_{\text{miss}} \leq$  11305 (MeV/c<sup>2</sup>)  
 corresponds to 130 MeV  $^{12}\text{C}$  excitation.

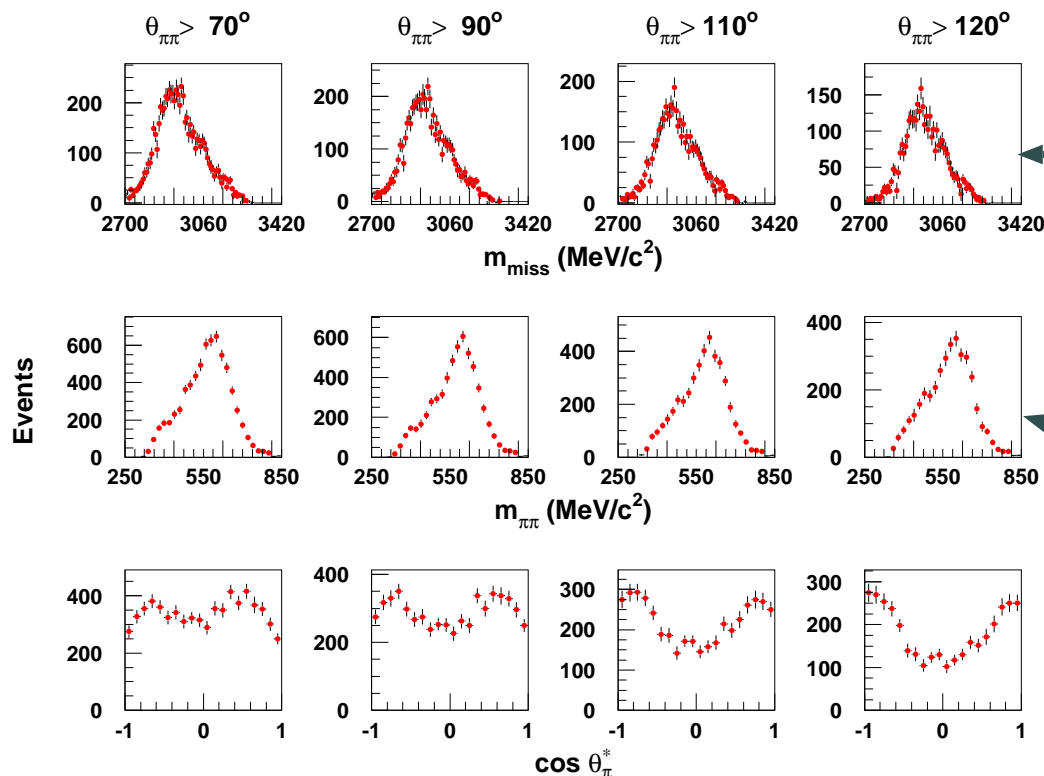


All simulations run for  $10^6$  TAGX triggers. y-axis labels indicate cut survival probability.

The mean cut survival probability of FSI processes is <25% of that of non-FSI processes, enhancing the expected relative proportion of non-FSI to FSI events by a factor of 4.

# The effects of the cuts upon the data

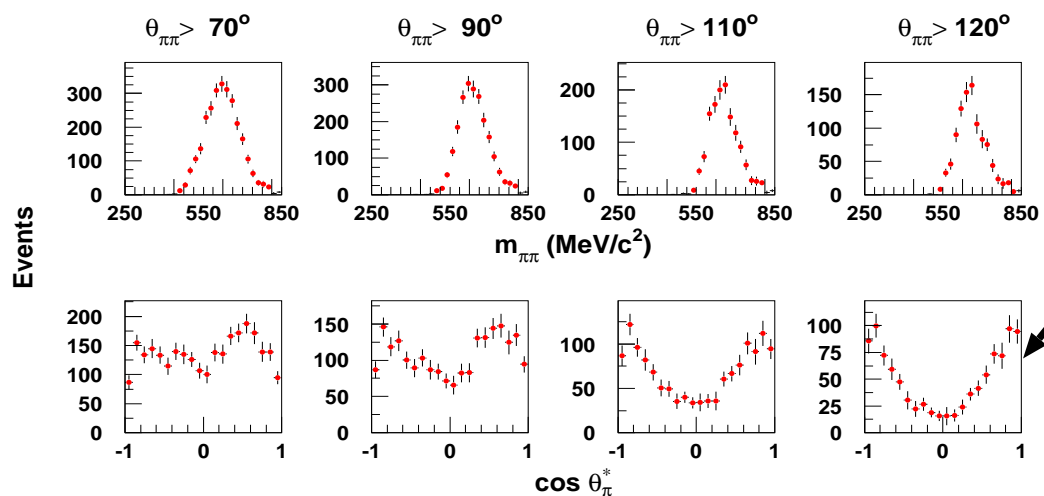
Opening angle cut only, i.e.  $3\pi$  events included.



Low  $m_{\text{miss}}$  region loses  $2\pi$  events with low relative momenta.

Invariant mass generally unaffected.

Opening angle and missing mass (110 MeV excitation) cuts.



No combination of  $\Delta\pi$ ,  $\Delta\Delta$ ,  $\sigma^0$  without  $\rho_L^0$  can reproduce shape and change of population of helicity angle data.

$^3\text{He}$ ,  $800 < E_\gamma \leq 960$  MeV data shown. Others similar.

# Results of cut-dependence study

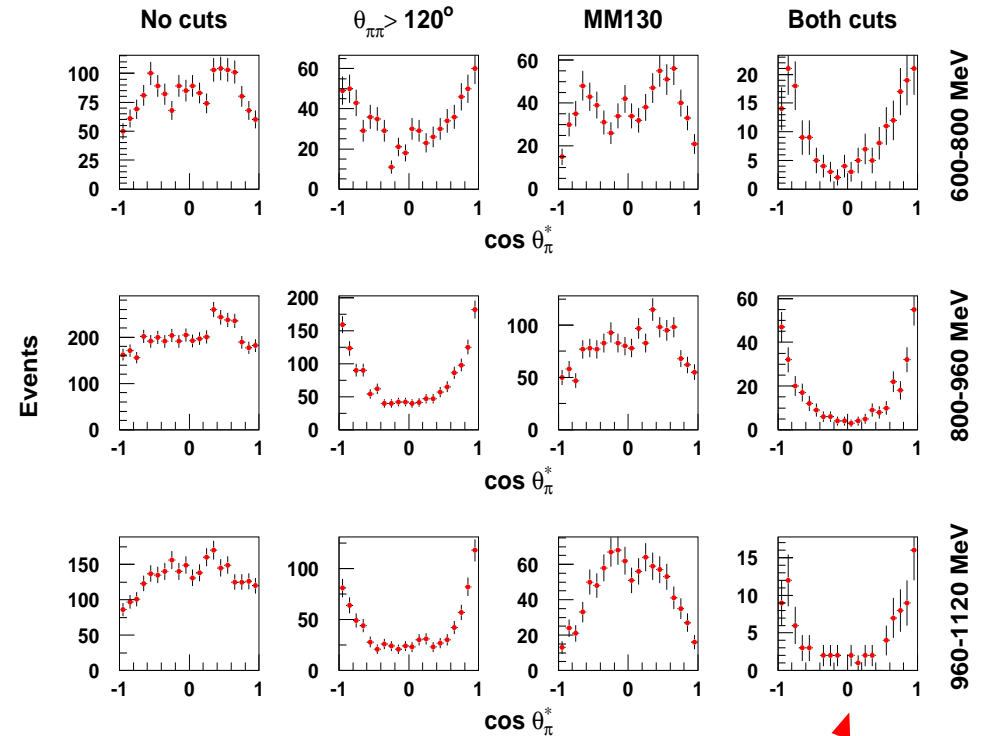
Data distributions for all three nuclei are similar, and respond similarly to the cuts.

Application of the opening angle cut removes most of the yield near  $\cos \theta_{\pi}^* = 0$ , resulting in  $p$ -wave-like distributions.

Application of only the missing mass cut eliminates events across the distributions, without altering their shapes.

Two-step processes, such as  $\Delta\pi$ ,  $\Delta\Delta$ ,  $N^*\pi$ , can not be the main contributors, as they have different responses to the cuts than the data do.

$^{12}\text{C}$  data distributions.



The small number of surviving events near  $\cos \theta_{\pi}^* = 0$  indicate that the total number of events from non- $\rho^0$  processes is small.

# Extraction of the In-Medium $\rho^0$ Invariant Mass Distribution

We may be able to use the helicity plots for the various invariant mass bins to study the in-medium  $\rho^0$  spectral function.

- Need to investigate the relative contributions of the various  $\pi^+\pi^-$  production processes to the observed  $\cos\theta_{\pi^+}^*$  distributions.
- Subtract the contributions of the background processes in as model-independent manner as possible.

⇒ The result is a better measure of the observed  $\rho_L^0$  distribution versus invariant mass for  ${}^2H$ ,  ${}^3He$ ,  ${}^{12}C$ .

- Fit the distributions with

$$Events = \mathbf{A} + \mathbf{B}\cos\theta_{\pi^+}^* + \mathbf{C}\cos^2\theta_{\pi^+}^*$$

This is not intended to provide a perfect fit to the data distributions, but rather a means to quantify the relevant features of the observed distributions.

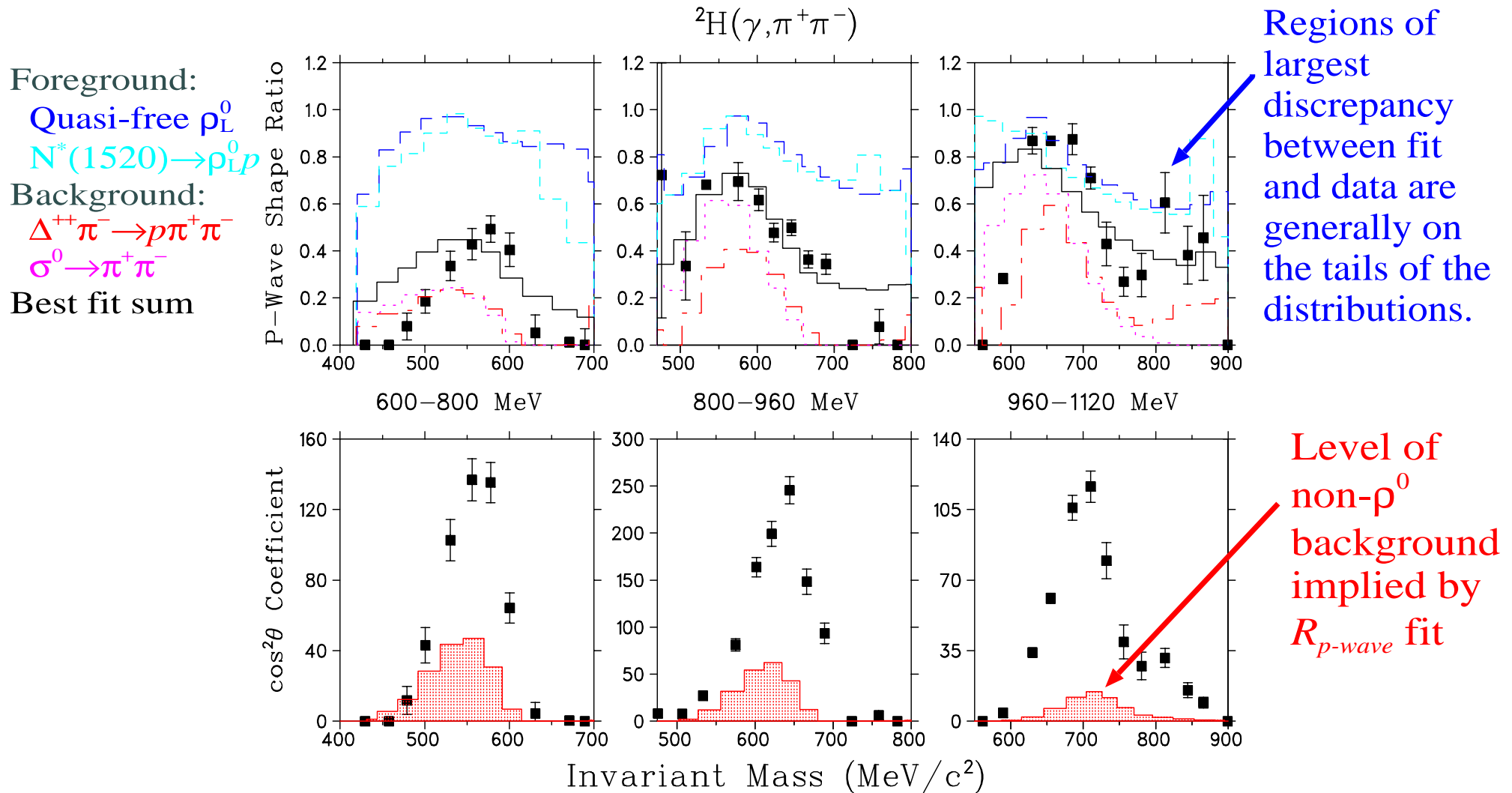
**A** - pedestal at  $\cos\theta_{\pi^+}^*$ . Indicative of non- $\rho_L^0$  contribution.

**B** - skewness coefficient.      **C** -  $p$ -wave coefficient.

- To characterize the data distributions, form  $p$ -wave shape ratio

$$R_{p\text{-wave}} = \frac{\mathbf{C}}{3|\mathbf{A}| + \frac{3}{2}|\mathbf{B}| + |\mathbf{C}|}$$

# Comparison of $p$ -wave shape ratios of data and simulations



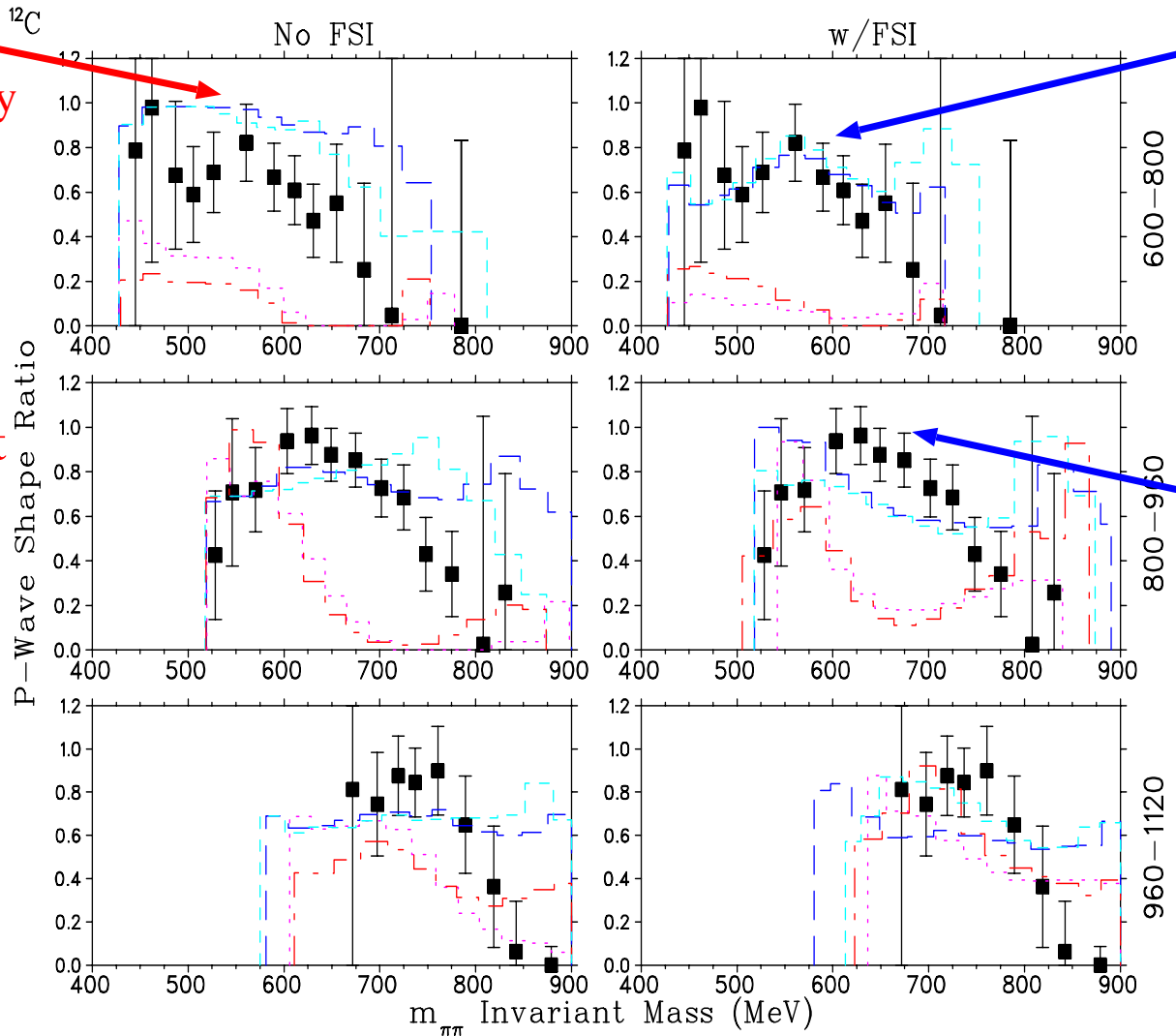
Data lie midway between ratios of foreground and background processes.

Effect of non- $\rho^0$  background is to dilute the  $p$ -wave ratio observed for the data.

The amount of observed dilution can be used to estimate the background present in the data.

# Helicity analysis estimate of $^{12}\text{C}$ FSI-corrections

Data  $p$ -wave ratios are degraded slightly from those of pure  $\rho_L^0$  processes.



Ratios consistent with  $<10\%$  background contribution.

Data and FSI- $\rho^0$  processes in good agreement. Likely fortuitous, as this implies a 0% background contribution.

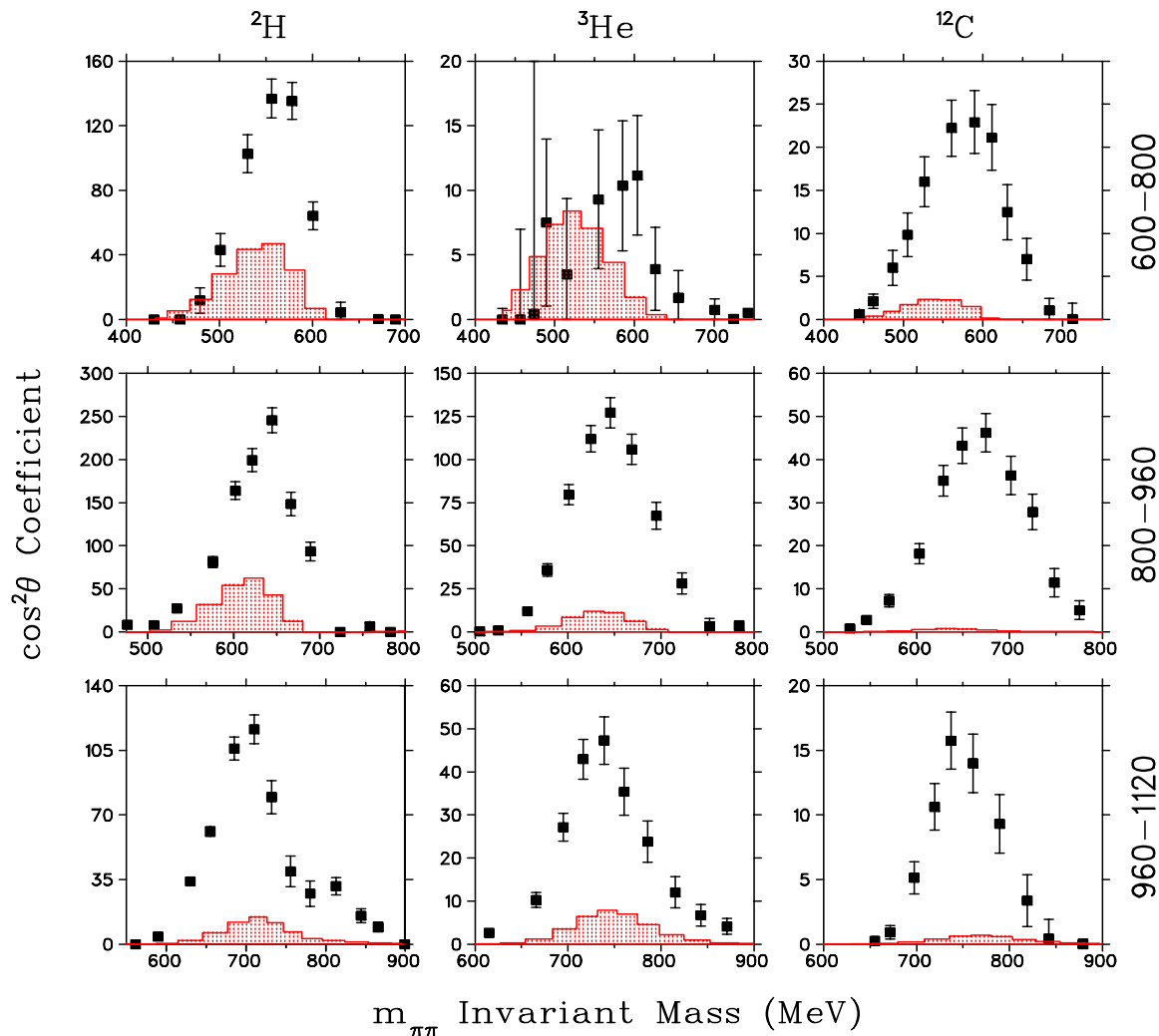
$R_{p\text{-wave}}$  of data exceeds those of FSI- $\rho^0$  MC.  $\Rightarrow$  Implies a **negative** number of background process events. **Unreasonable!**

We expect most rescattering FSIs have been removed by the analysis cuts.  $\Rightarrow$  Since rescattering processes do not significantly affect the  $p$ -wave ratio, their contributions are relatively difficult to distinguish.

The assumption of no rescattering FSIs leads to the subtraction of more non- $\rho_L^0$  background, and so is the more conservative of the two choices.

Foreground:  
 Quasi-free  $\rho_L^0$   
 $N^*(1520) \rightarrow \rho_L^0 p$   
 Background:  
 $\Delta^{++} \pi^- \rightarrow p \pi^+ \pi^-$   
 $\sigma^0 \rightarrow \pi^+ \pi^-$   
 Best fit sum

# Subtraction of background to yield the in-medium $\rho_L^0$ invariant mass distribution



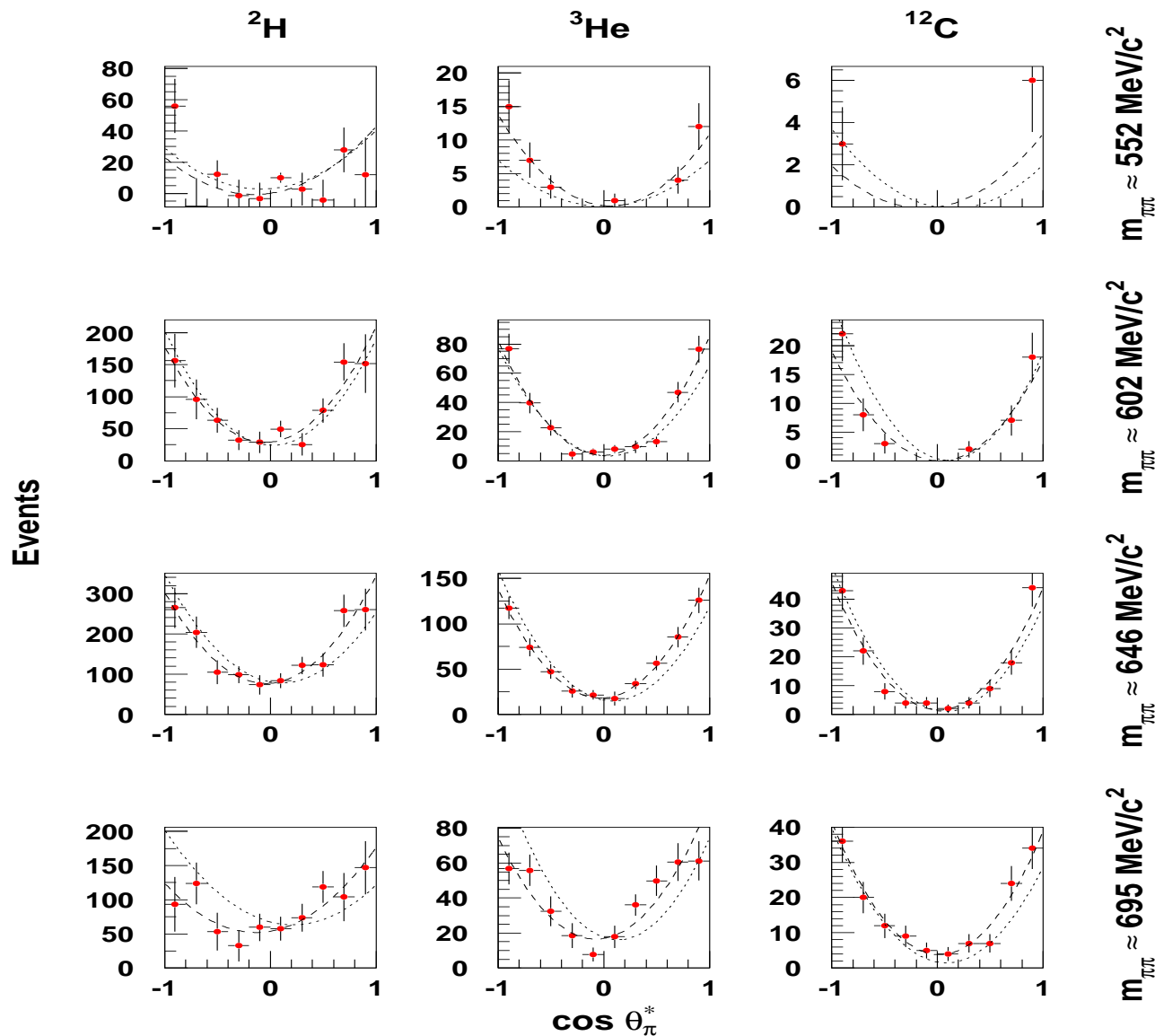
Relative proportion of foreground processes [quasi-free  $\rho_L^0$  and  $N^*(1520) \rightarrow p\rho_L^0$ ], after all cuts, as determined from fitting the  $R_{p\text{-wave}}$  distributions to the data.

Nucleus	Tagged photon energy bin (MeV)		
	600-800	800-960	960-1120
$^2\text{H}$	$0.66 \pm 0.06$	$0.75 \pm 0.04$	$0.87 \pm 0.06$
$^3\text{He}$	$0.25 \pm 0.11$	$0.91 \pm 0.02$	$0.83 \pm 0.05$
$^{12}\text{C}$	$0.90 \pm 0.01$	$0.98 \pm 0.02$	$0.96 \pm 0.14$

$$\rho_L^0(m_{\pi\pi}, E_\gamma) \text{ Distribution} = C_{\text{data}} - (1 - \eta_\rho) C_{\text{background}}$$

Average of  $\Delta\pi$  and  $\sigma^0$  MCs

# Is this analysis internally consistent?



$800 < E_{\gamma} \leq 960 \text{ MeV}$  data.  
 [Long-dash] fit to data.  
 [Short-dash] coefs from  
 fit to  $R_{p\text{-wave}}$  distributions.

The consistency of the two curves, within data error bars, indicates the validity of the  $p$ -wave shape ratio analysis.

# Comparison of extracted in-medium distributions to model calculations

A number of significant effects must be taken into account before any comparison can be made:

1. Subthreshold experiment:
  - ⇒ Limited kinematic phase space effects must be taken into account.
2. TAGX spectrometer acceptance and detection threshold effects are significant.
3. Model must be subjected to same  $\theta_{\pi\pi}$  and  $m_{miss}$  cuts as the experimental data.

The best way to take these effects into account is to embed the model calculation within a MC simulation of the experiment, and analyze the simulated events in the same manner as the data.

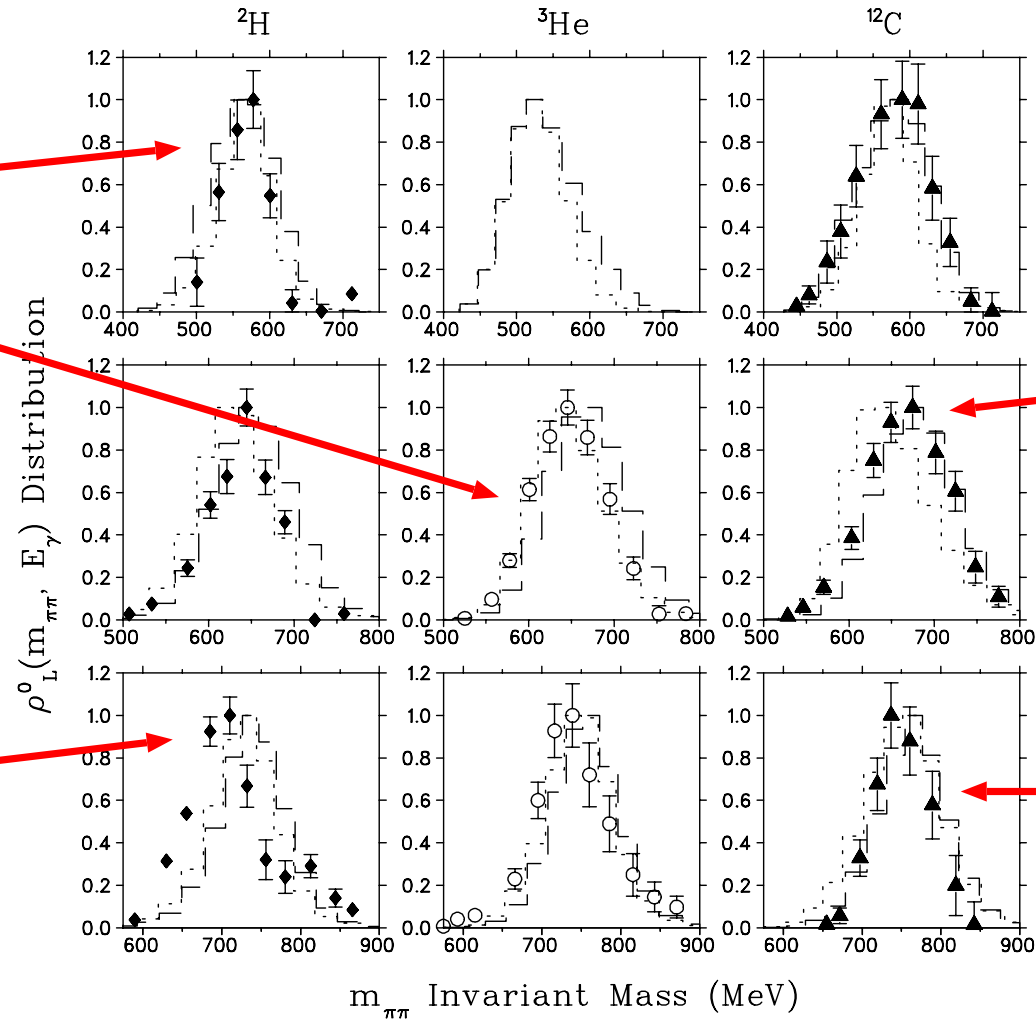
⇒ **This is the only reliable manner in which model comparisons can be made to the data.**

1. Kinematic models:
  - ⇒ Quasi-free  $\rho_L^0$  production.
  - ⇒ Quasi-free  $N^*(1520) \rightarrow \rho^0 p$ .
2. Phenomenological models:
  - ⇒ Relativistic Resonance Model.
  - ⇒  $\rho - N$  Interaction “Rhosobar” Model.
  - ⇒ Quark Meson Coupling Model.

# Comparison to free $\rho^0$ line shape in kinematic model

Light nuclei  
more consistent  
with  $N^*(1520)$   
model.

Model centroids  
too high by  
 $\sim 40$  MeV.



[Long-dash] Quasi-free  $\rho_L^0$   
[Short-dash]  $N^*(1520) \rightarrow \rho_L^0 p$

Carbon agrees  
better with  
quasi-free  $\rho_L^0$   
model.

$\rho_L^0$  distribution  
is slightly  
broader than  
data and peaked  
at higher  $m_{\pi\pi}$ .

$\rho^0$  shape taken from partial wave analysis of  
 $e^+e^- \rightarrow \pi^+\pi^-$  data from  $2m_\pi$  to  $m_\eta$ .  
 $\Rightarrow$  M. Benayoun et al., Z. Phys. **C58** (1993) 31.  
**Shapes are the same in both models, but the  
effects of kinematic phase space and Fermi  
momentum are different.**

MC-simulated  $\rho^0 \rightarrow \pi^+\pi^-$  are tracked  
through the experimental apparatus;  
 $m_{\pi\pi}$  distributions reconstructed  
via helicity analysis.

## Conclusions from comparison to kinematic models

- The general agreement of the experimental distributions with expectations from partial wave analysis verify that the helicity analysis has indeed identified pions originating from  $\rho^0$  decay.
- The  ${}^2H$  and  ${}^3He$  data distributions favor  $\rho_L^0$  production via the quasifree  $N^*(1520) \rightarrow \rho_L^0 N$  mechanism.
  - ⇒ This provides strong experimental support of the likely  $\rho_L^0$  production mechanism at these photon energies.
- The lack of evidence in the  ${}^{12}C$  data to support even modest  $N^*(1520)$  could be due to the role the  $N^*(1520)$  plays in nuclei.
  - ⇒ Ongoing debate re. in-medium  $N^*(1520)$  mass and width.
- A detailed comparison of the data with the simulations reveal deviations which may be due to higher  $N^*$  and  $\Delta$  resonances and/or reaction mechanism admixtures.
  - ⇒ Comparison with the phenomenological models may shed further light on these discrepancies.

## Saito-Tsushima-Thomas (STT) Quark Meson Coupling Model

- Quarks in non-overlapping nucleon bags interact self-consistently with both scalar and vector mesons in the mean-field approximation.
- The vector mesons are described by quark bags utilizing the MIT bag model.
- The in-medium masses are given in terms of the mean-field value of the  $\sigma$  meson at the local nuclear density.

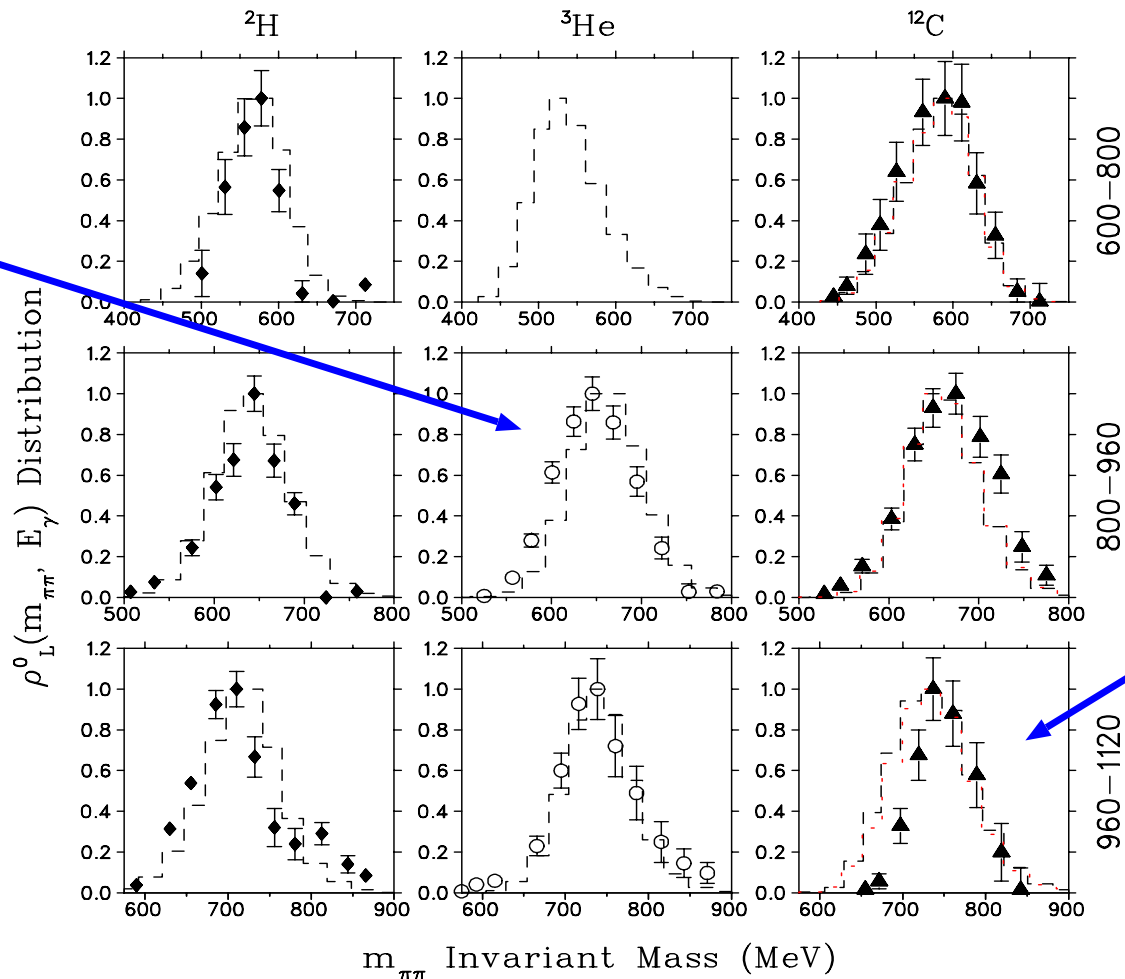
$$m_{\rho}^* = m_{\rho} - \frac{2}{3}(g_{\sigma}\sigma)\left[1 - \frac{8.58 \times 10^{-4}(\text{MeV}^{-1})}{2}(g_{\sigma}\sigma)\right]$$

- The model describes the modification of the  $\rho^0$  mass due to nuclear binding effects only, and can make no statement on any  $\rho^0$  width or shape modification.  
 $\Rightarrow$  in the MC implementation, the free PDG width and shape of the  $\rho^0$  was used.
- This is the only work to provide specific predictions for our experiment.  
 $\Rightarrow$  Predict a 40 MeV reduction in the mass of the  $\rho^0$  in  ${}^3\text{He}$ .

[K. Saito, K. Tsushima and A.W. Thomas, PRC **56** (1997) 566]

The agreement of the Saito-Tsushima-Thomas model with the data is impressive, given its' lack of any in-medium  $\rho^0$  width or shape modification.

Data centroid is shifted by additional 20 MeV, over model prediction of 40 MeV shift.



Only model to underpredict centroid of this distribution.

STT model agreement with the observed  $\rho^0$  width implies that the  $\rho_L^0$  line shape is largely unaffected by the nuclear medium.

⇒ Consistent with the kinematic models.

## Rapp-Chanfray-Wambach (RCW) $\rho - N$ Interaction “Rhosobar” Model

- $\rho^0$  rescattering and particle-hole excitation in the medium lead to an enhancement of the  $m_{\pi\pi}$  distribution below 600 MeV/c<sup>2</sup> and a depletion of the top of the  $\rho^0$  invariant mass peak.
  1. Medium modification due to the interaction of the  $\rho^0$  with intermediate two-pion states.
  2. Significant contributions from “rhosobar” processes such as



due to the large  $\rho NN$  and  $\rho N\Delta$  coupling constants, and the significant branching ratios of  $N^*(1720)$  and  $\Delta(1905)$  decays to  $\rho N$  final states.

⇒ Spectral function constrained by low  $m_{\pi\pi}$  PWA and timelike  $F_\pi$  parameterization.

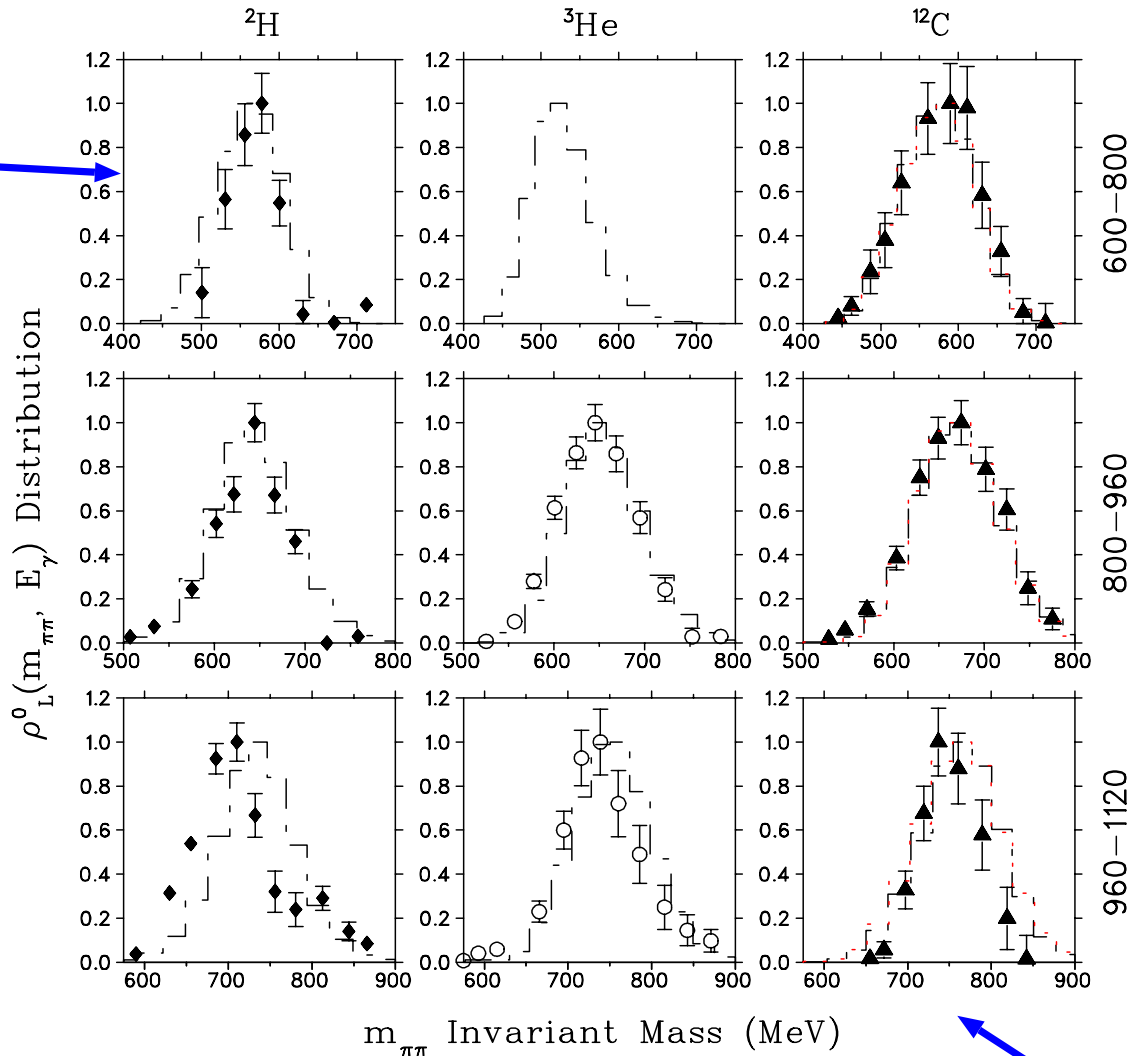
- RCW model accounts very well for the high energy heavy ion dilepton spectra, and so provides an alternate explanation to that of the chiral phase transition.

[R. Rapp, G. Chanfray, J. Wambach, NP A **617** (1997) 472]

- In-medium  $\rho$  spectral functions appropriate to cold nuclear matter are incorporated into a MC model of the quasi-free  $A(\gamma, \rho^0)pX$  reaction.

# The Rapp-Chanfray-Wambach model provides a good description of the data over the full energy range and for all three nuclei.

Discrepancies with deuterium data may be due to its high core density. Exceeds limit of provided spectral functions.



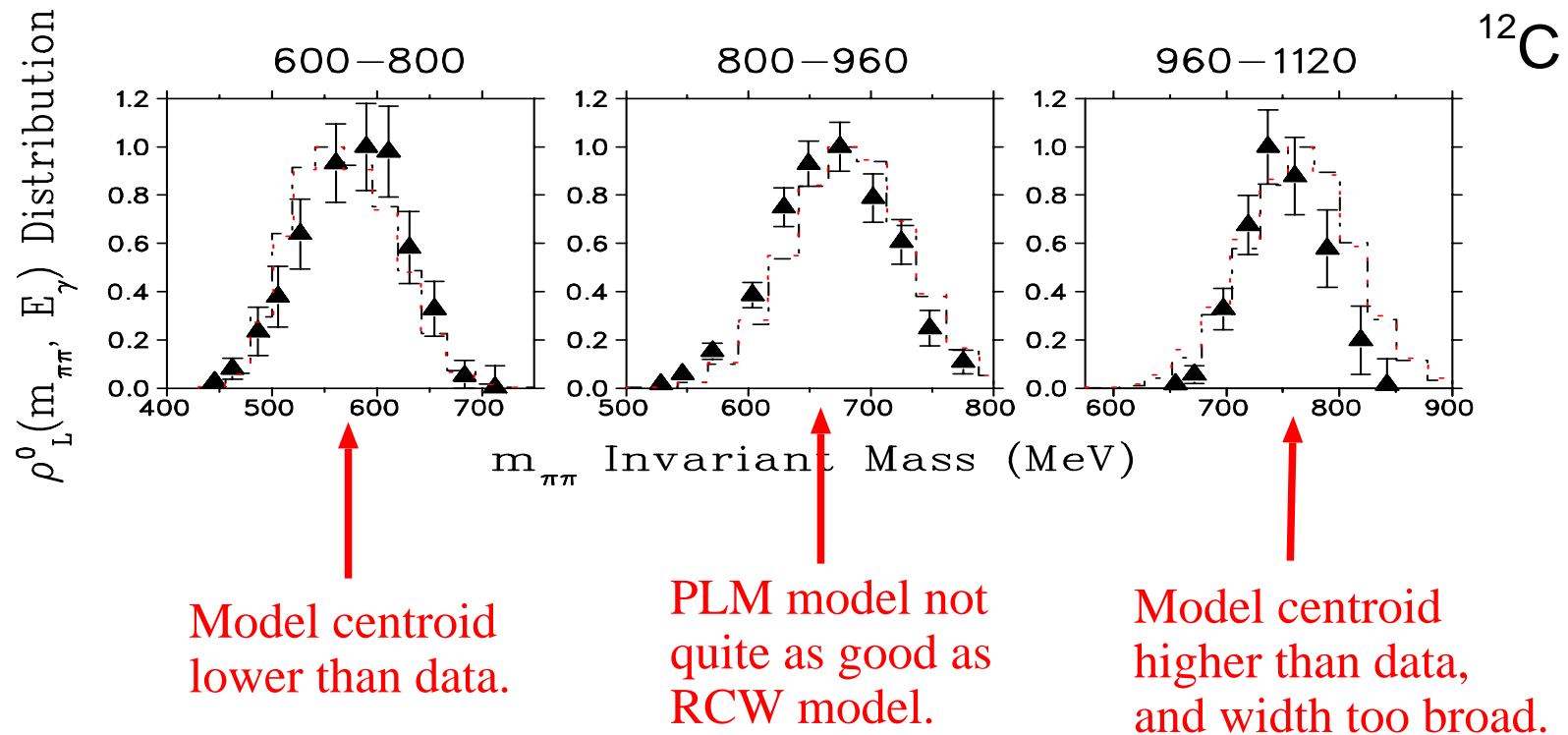
Agreement with the data is worst for the 960–1120 MeV bin for all three nuclei.

# Post-Leupold-Mosel (PLM) Relativistic Resonance Model

$\rho^0$  rescattering in nuclear matter, calculated using the low-density approximation.

- ⇒ In-medium self-energy of the  $\rho^0$  is completely determined by the  $\pi N$  forward scattering amplitude, extracted from  $\pi N \rightarrow \pi \pi N$  processes.
- ⇒ In the longitudinal channel, the  $N^*(1520)$  is the main contributor.
- ⇒  $N^*(1520) \rightarrow N\rho \approx 25\%$  branching ratio.
- ⇒ Since  $m_N + m_p > 1520$  MeV (assuming  $m_p = 770$  MeV), the decay can only proceed via the lower mass component of the  $\rho$  spectral function.

[M. Post, S. Leupold, U. Mosel, NP A **689** (2001) 753]



## Conclusions from comparison to phenomenological models

- Rapp-Chanfray-Wambach model provides a reasonable description of the data from all 3 nuclei over all energy bins.
  - ⇒ Simulated invariant mass distributions exhibit some characteristics of the  $\rho^0$  and  $N^*(1520)$  simulations.
  - ⇒ Presumably a reflection of the “rhobar” nature of the model.
- Post-Leupold-Mosel model simulations are similar to RCW.
  - ⇒ While RCW tracks the changing shape of the  $^{12}C$  distribution with energy, the PLM model predicts a larger energy dependence than the data portray.
- Saito-Tsushima-Thomas model does a surprisingly good job of describing the data.
  - ⇒ Underpredicts the  $^3He$  mass shift at  $800 < E_\gamma \leq 960$  MeV by 20 MeV.
  - ⇒ Only model to underpredict  $^{12}C$  mass at  $960 < E_\gamma \leq 1120$  MeV.
- **It might seem reasonable that the combination of the STT and RCW-PLM models will together provide a good description of the data.**
  - i.e. a central mass shift in addition to a spectral function modification.**
- A similar argument has already been raised by Brown and Rho in the context of recent result from RHIC [nucl-th/0206021].
  - ⇒ Brown-Rho scaling of medium-dependent masses is combined with the spectral function modification of RCW in a unified picture.

## $\mathbf{A}(\gamma, \pi^+\pi^-)$ Helicity Analysis Summary

- Significant  $\rho \rightarrow \pi^+\pi^-$  decay with  $l = 1, m = 0$  is observed for  $575 \leq m_{\pi\pi} \leq 750$  MeV on  ${}^2H, {}^3He, {}^{12}C$ .
- We employed this unique signature to isolate  $\rho_L^0$  events in the 600-1120 MeV photon energy region.
  - $\Rightarrow \cos\theta_\pi^*$  distributions fit with  $A + B\cos\theta + C\cos^2\theta$  versus  $m_{\pi\pi}$ .
  - $\Rightarrow$  After subtraction of a small non- $\rho$  background, coefficient  $C$  was used to yield in-medium  $\rho_L^0$  invariant mass distributions for all three nuclei over three bins of tagged photon energy.
- free  $\rho^0$  line shape from  $e^+e^- \rightarrow \pi^+\pi^-$  partial-wave analysis incorporated into quasi-free kinematic MC simulations and compared with the data.
  - $\Rightarrow$  600-960 MeV  ${}^2H$  data favor production via the  $\gamma N_F \rightarrow N^*(1520) \rightarrow \rho_L^0 N'$  production mechanism.
  - $\Rightarrow$  For the  $960 < E_\gamma \leq 1120$  MeV data, neither of the kinematic production mechanism models account for the observed distribution.

## $\mathbf{A}(\gamma, \pi^+ \pi^-)$ Helicity Analysis Summary

- $\rho_L^0$  spectral functions from relativistic rescattering, rho-sobar, and quark-meson coupling models incorporated into quasi-free MC simulations and compared with the data.
  - ⇒ Comparison with the STT model simulation, using the free  $\rho_L^0$  width and line-shape indicates that the data provide no evidence of an in-medium  $\rho_L^0$  distribution that is broader than the free distribution.
    - \* This is consistent with model expectations, which predict that the in-medium  $\rho_T^0$  distribution will be significantly wider than the  $\rho_L^0$  distribution.
  - ⇒ STT model predicts a modified mass of 730 MeV in  ${}^3He$ , in excellent agreement with the 960-1120 MeV data. For the 800-960 MeV bin, the data support a somewhat lower mass,  $m_\rho^* = 700 - 710$  MeV.
  - ⇒ RCW model is in excellent agreement with the data for the two lower energies, but RCW predicts a wider distribution in the 960-1120 region than the data support.
- A model which incorporates both the nuclear binding effect of STT as well as the spectral function modifications of RCW-PLM has the potential to provide the best description of the  ${}^{12}C$  data.
- Look forward to new data forthcoming from GSI-HADES.